Journal of the Indian Institute of Science
A Multidisciplinary Reviews Journal
ISSN: 0970-4140 Coden-JIISAD

REVIEWS

Non-Equilibrium Dynamics in Ultracold Atoms: A Projection Operator Approach

K. Sengupta

Abstract | In this article we provide a brief pedagogical introduction to the physics of the Bose-Hubbard model near its superfluid-insulator transition. We focus on the properties of the system near this quantum critical point in the presence of an external drive which constitutes a ramp of the hopping strength J of the bosons with a fixed rate τ^{-1}. We provide an introduction to the projection operator method which can treat such non-equlibrium dynamics of the model beyond mean-field theory and discuss its relevance for current experiments.

1 Introduction

Ultracold bosonic atoms in optical lattices provide us with an unique setup to study properties of bosons near a Mott insulator-superfluid (MI-SF) quantum critical point.[1,2] Such systems are well known to be described by the Bose-Hubbard model.[3] This model described by the Hamiltonian

$$\mathcal{H} = T + H_0, \quad T = \sum_{\langle \mathbf{r}\mathbf{r}' \rangle} -J b^\dagger_{\mathbf{r}} b_{\mathbf{r}'}$$
$$H_0 = \sum_{\mathbf{r}} \left[-\mu \hat{n}_{\mathbf{r}} + \frac{U}{2} \hat{n}_{\mathbf{r}} (\hat{n}_{\mathbf{r}} - 1) \right] \quad (1)$$

where $b_{\mathbf{r}}$ ($\hat{n}_{\mathbf{r}}$) is the boson annihilation (number) operator living on site $\mathbf{r}$ of a d-dimensional lattice with coordination number z, and the chemical potential μ fixes the total number of particles. This model has already been theoretically studied using both analytical[4–6] and numerical[7] techniques. The presence of such an experimental test bed has led to a plethora of new theoretical studies on the model.[8–11] Most of the initial analytical studies have concentrated on obtaining the phase diagram of the model by using mean-field theory,[4,5] excitation energy computation,[6] and strong-coupling expansion for the boson Green function.[11] The results obtained by these methods have been compared to quantum Monte Carlo (QMC) data.[7,10] Out of these methods, the strong-coupling expansion[11] (excitation energy computation[6]) and the NPRG approach[9] provide the closest numerical match to QMC data in 2D (3D); however, the qualitative picture of the equilibrium property of the transition.

Recently, it has been realized that such ultracold bosonic systems also allow us easy access to the non-equilibrium dynamics of its constituent atoms near the MI-SF quantum critical point. The theoretical study of such quantum dynamics on various models has seen great progress in recent years.[12] Most of these works have either restricted themselves to the physics of integrable and/or one-dimensional (1D) models or concentrated on generic scaling behavior of physical observable for sudden or slow dynamics through a quantum critical point.[12–16] However quantum dynamics of specific experimentally realizable non-integrable models in higher spatial dimensions and strong coupling regime has not been studied extensively mainly due to the difficulty in handling quantum dynamics of plethora of states in the system's Hilbert space. The Bose-Hubbard model with on-site interaction strength U and nearest neighbor hopping amplitude J, which provides an accurate description for ultracold bosons in an optical lattice, constitutes an example of such models. Most of the studies on dynamics of this model have concentrated on $d = 1$,[18] weak coupling regime,[19] and mean-field order parameter dynamics following a sudden ramp in the strong coupling regime.[20–22] Recent experiments[2] clearly necessitate computation of dynamical evolution of several other quantities in higher dimensional Bose-Hubbard model in the strong-coupling regime ($U \gg J$) beyond the mean-field theory and for arbitrary ramp time τ. However, none of the works mentioned above presents an analysis of the non-equilibrium dynamics of the model beyond mean-field theory.

Theoretical Physics Department, Indian Association for the Cultivation of Science, Jadavpur, Kolkata-32, India.

ksengupta1@gmail.com

More recently, the authors of Ref. 23 have developed a theoretical formalism which enables one to analyze the dynamics of the Bose-Hubbard model beyond mean-field theory near the MI-SF critical point.[23] The method uses a projection operator technique which enables us to account for the quantum fluctuations over the mean-field theory perturbatively in $J_f/U(J(t)/U)$ and therefore yields accurate results as long $J_f/U(J(t)/U) \ll 1$ for sudden(ramp) dynamics. This allows one to treat sudden and slow ramps at equal footing near the MI-SF quantum critical point. As shown in Ref. 23, the projection operator method yields an accurate phase diagram and also provides an estimate of dynamically generated defect density which shows a qualitatively reasonable match with recent experimental results.[2]

In this article, we would aim to provide a pedagogical introduction to the dynamics of the Bose-Hubbard model using projection operator method. To this end, we first provide a brief introduction to the Bose-Hubbard model in Sec. 2. This will be followed by a detailed exposition of the projection operator method in Sec. 3.

2 Bose-Hubbard Model: A Brief Introduction

The physics of bosons has the fascinating theoretical aspect called Bose-Einstein condensation (BEC), *i.e.*, occupation of a single quantum state by macroscopic number of bosons at low enough temperature leading to fascinating phenomenon such as superfluidity. Moreover, there has been renewed interest in physics of these systems due to their recent experimental realizations in trapped atoms.[1] Such experiments can manipulate BECs with incredible precision. In particular, it has been possible to form an optical lattice in a system of these trapped bosons, which, when deep enough, may result in Mott localization of Bosons leading to destruction of the BEC state. Such a destruction is a result of a phase transition in the bosonic system. The physical temperatures relevant in these experiments are of the order of tens of nanokelvins (which makes these systems the coldest known place in the universe) and is at least $2-3$ order of magnitudes lower than all other energy scales. Thus such a transition is an example of a quantum phase transition. In this section we shall give a brief account of the physics associated with such a transition, by considering the simplest possible BECs, *i.e.*, BECs formed from spin-less bosonic atoms such as ^{87}Rb.

The optical lattice is formed by applying six counter-propagating laser beams of fixed wavelengths to the condensed Bose atoms in a trap(which can be magnetic or optical). These lasers have a electric field $\mathbf{E}$ and form standing waves of light in all three directions. The atoms have a polarizibility $\alpha(\omega;\omega_0)$, where ω is the applied laser's frequency and ω_0 is some characteristic frequency of the atoms. As a result, the atoms feel a potential $V = -\alpha(\omega;\omega_0)|E|^2$. By tuning the frequency of the applied laser, one can now make α positive, so that the atoms have a tendency to sit at the bottom of the potential which acts as lattice sites. Once they do that, the kinetic energy of the atoms makes them hop from one site to the next. As the lattice becomes deeper, this process is exponentially suppressed since it can be shown that the hopping amplitude $J \sim \exp(-\sqrt{V/E_R})$, where $E_R = \hbar^2/2m\lambda^2$, called the recoil energy, is the basic energy scale created out of the mass(m) of the atoms and the wavelength(λ) of the laser. The bosons which form the condensate is neutral and so the interaction between them is short-range Van-der-Walls type. In the presence of a lattice, the interaction between the boson is most significant when they are on the same lattice site which we shall call U. Interaction between the atoms in the neighboring site can be neglected as a first approximation. The key point to recognize is that this interactions, unlike the hopping strength J, do not depend exponentially on the strength of the lattice potential V.

Now consider the an optical lattice with one boson per site. If the kinetic energy is large compared to the on-site interaction ($J \gg U$), the bosons are free to hop around and therefore the ground state of the system is clearly the one in which a major number of bosons sit in the $k = 0$ state. Thus the bosons form a BEC. However, if we now increase the depth of the lattice J/U becomes small, and hence a stage comes when the bosons do not find it convenient to hop around since they have to pay too much interaction energy cost to do so. In this limit all the bosons become localized. Since this localization is induced by interaction, its called a Mott insulating state.

How do we see this transition experimentally? It turns out the easiest way to look at this bosons is to switch at the lattice and the trap at the same time and let the bosons fly out. After some time of such free flight, the position distribution of these bosons can be measured by absorption imaging of the bosons in a free flight. Since the position of the bosons after a time t of such a flight depends on their starting velocity or equivalently momentum, *the position distribution of these bosons actually reflect their momentum distribution inside the trap*. Now if there were no lattice, all the bosons

would be in the $k = 0$ state (the condensate) and hence their momentum distribution will be localized around $k = 0$. On the other hand, if the bosons were in the Mott state, they are localized in real space which means their momentum can take all possible values. Thus the Mott state momentum distribution should reflect a featureless blur. As the strength of the optical lattice is increased, it is therefore expected that the momentum distribution of the bosons will crossover from a central peaked one to a featureless blurred one. This is precisely what is seen in experiments.[1] The phase transition occurs somewhere around $V_0 \simeq 14E_R$ where the central bright spot disappears.

To develop a simple theory for this transition, let us first look at the Mott* state when $J \ll U$ and there is an integer number of bosons per site. Neglecting the effect of hopping of bosons here, we can see that the Hamiltonian is

$$H_{\rm Mott} = U\sum_i \frac{1}{2}n_i(n_i-1) - \frac{\mu}{U}n_i \tag{2}$$

Since the Hamiltonian is on-site one could easily find out the ground state wavefunction and energy. This state is given by

$$\begin{aligned}\Psi_{\rm ground} &= \prod_i |n_i \\ &= n_0 > \frac{E[n_0]}{U} = \frac{1}{2}n_0(n_0-1) - \frac{\mu}{U}n_0\end{aligned} \tag{3}$$

where $n_0 \equiv n_0(\mu/U)$ is the integer which minimizes $E[n_0]$. One can easily check that

$$\begin{aligned} n_0 &= 0 \quad \text{for } \mu \le 0 \\ &= 1 \quad \text{for } 0 \le \mu \le U \\ &= 2 \quad \text{for } U \le \mu \le 2U.... \end{aligned} \tag{4}$$

The Mott† state is the stable ground state when $J/U \ll 1$. The next question to ask is what happens when we increase t. From the experiments, we already know the answer; the ground state becomes unstable when a critical J is reached. Now to find when the ground state is destabilized, we need to find out what are the possible excited states of the system over the ground state and when can they destabilize the ground state. At finite J, the excited state which corresponds to addition of an extra particle/hole over the Mott ground state with n_0 particles per site has a minimum excitation energy given by

$$\begin{aligned}\delta E_p &= -\mu + Un_0 - zJ(n_0+1) \\ \delta E_h &= \mu - U(n_0-1) - zJn_0\end{aligned} \tag{5}$$

which destabilizes the Mott ground state at

$$J_c^p = \frac{-\mu + Un_0}{z(n_0+1)} \quad J_c^h = \frac{\mu - U(n_0-1)}{zn_0} \tag{6}$$

leading to a critical hopping of $J_c = {\rm Min}[J_c^p, J_c^h]$. The simple estimate of J_c as outlined above captures some essential features of the transition. First, we note that at the boundary between the Mott phases with n_0 and $n_0 + (-)1$ particles, $\mu = Un_0(n_0-1)$ so that J_c vanishes. At these points the excited state energies $\delta E_p(\delta E_h)$ vanishes for $J_c^p(J_c^h) \simeq 0$ and there is no Mott state. Second at the tip of the Mott lobe, where $J_c^p = J_c^h = (2n_0+1)/z$ and $\mu = 2n_0(n_0+1)/z(2n_0+1)$, it becomes equally costly to add a particle or a hole to the system. In other words, the system possess particle-hole symmetry at this special point. This property has profound consequence on the universality class of this phase transition which we shall not dig into in details in the present lecture. More refined calculations such as a mean-field analysis and even those which keep track of higher order fluctuations has been carried out in the literature and we shall discuss this later. The qualitative symmetry issues that we have discussed above, however, do not change.

3 Projection Operator Method

The Hamiltonian of the Bose-Hubbard model is given by Eq. 1. The corresponding many-body Schrödinger equation $i\hbar\partial_t|\psi\rangle = \mathcal{H}|\psi\rangle$ is difficult to handle even numerically due to the infinite dimensionality of the Hilbert space. A typical practice is to use the Gutzwiller ansatz $|\psi\rangle = \prod_{\mathbf{r}}\sum_n c_n^{(\mathbf{r})}|n\rangle$, and solve for $c_n^{(\mathbf{r})}$ keeping a finite number of states n around the Mott occupation number $n = \bar{n}$. This yields the standard mean-field results with $c_n^{(\mathbf{r})} = c_n$ for homogeneous phases of the model.

To build in fluctuations over such mean-field theory, we use a projection operator technique.[24] The key idea behind this approach is to introduce a projection operator $P_\ell = |\bar{n}\rangle\langle\bar{n}|_{\mathbf{r}} \times |\bar{n}\rangle\langle\bar{n}|_{\mathbf{r}'}$ which lives on the link ℓ between the two neighboring sites $\mathbf{r}$ and $\mathbf{r}'$. The hopping term of $\mathcal{H}$

*Note that starting from perfect Mott state at $J = 0$ where $f_1 = 1$ and $f_{n\neq 1} = 0$ does not lead to any dynamics since all fields in the right side of Eq. 10 except $\chi_n(\mathbf{r})$ vanishes leading to a trivial phase-only contribution to f_1. This property can be seen to be a consequence of conservation of n at all sites for any $J(t)$.

†We note that $d + z = 4$ at the tip of the Mott lobe so that we are exactly at the upper critical dimensional of theory. The value of ν is thus expected to deviate from its mean-field value $1/2$ due to usual logarithmic corrections associated with critical theories at their upper critical dimensions. Its precise value for the Bose-Hubbard model remain uncertain; see for example B. Capogrosso-Sansone, B. V. Svistunov, and N.V. Prokofiev, Phys. Rev. B 75, 134302 (2007).

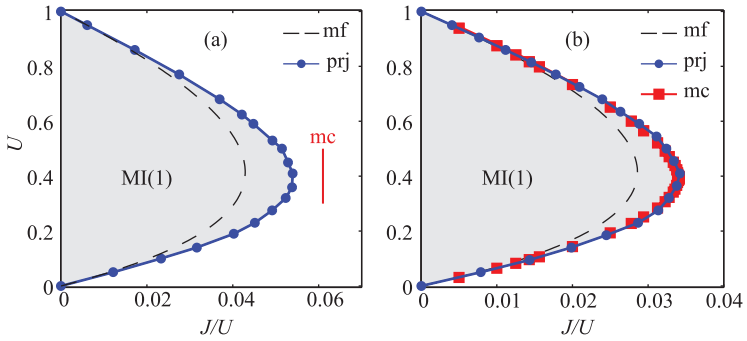

Figure 1: (Color online) Phase diagram of the Bose-Hubbard model in 2D (a) and 3D (b). The blue dots and blue solid lines (black dashed line) indicate the phase diagram obtained by the projection operator (mean-field) method. The red squares indicate QMC data.

can then be written as $T = \sum_{\langle \mathbf{r}\mathbf{r}'\rangle} -Jb^\dagger_{\mathbf{r}} b_{\mathbf{r}'} = \sum_\ell T_\ell = \sum_\ell [(P_\ell T_\ell + T_\ell P_\ell) + P^\perp_\ell T_\ell P^\perp_\ell]$, where $P^\perp_\ell = (1 - P_\ell)$. Note that in the strong-coupling regime, the term $T^0_\ell[J] = (P_\ell T_\ell + T_\ell P_\ell)$ represents hopping processes which takes the system out of the low-energy manifold.[24] We now devise a canonical transformation via an operator $S \equiv S[J] = \sum_\ell i[P_\ell, T_\ell]/U$ which eliminates $T^0_\ell[J]$ up to first order in zJ/U, where $z = 2d$ is the coordination number of the lattice, and leads to the effective Hamiltonian $H^* = \exp(iS)\mathcal{H}\exp(-iS)$ to $\mathrm{O}(z^2J^2/U)$

$$H^* = H_0 + \sum_\ell P^\perp_\ell T_\ell P^\perp_\ell - \frac{1}{U}\sum_\ell \times \Big[P_\ell T^2_\ell + T^2_\ell P_\ell - P_\ell T^2_\ell P_\ell - T_\ell P_\ell T_\ell\Big] - \frac{1}{U}\sum_{\langle \ell\ell'\rangle}\Big[P_\ell T_\ell T_{\ell'} - T_\ell P_\ell T_{\ell'} + \frac{1}{2}\Big(T_\ell P_\ell P_{\ell'} T_{\ell'} - P_\ell T_\ell T_{\ell'} P_{\ell'}\Big) + \mathrm{h.c.}\Big] \quad (7)$$

where H_0 denotes the on-site terms in Eq. 1. Using H^* one can now compute the ground state energy $E = \langle\psi|\mathcal{H}|\psi\rangle = \langle\psi'|H^*|\psi'\rangle + \mathrm{O}(z^3J^3/U^2)$, where $|\psi'\rangle = \exp(iS)|\psi\rangle$, and we use a Gutzwiller ansatz $|\psi'\rangle = \prod_{\mathbf{r}} \sum f^{(\mathbf{r})}_n |n\rangle$, so that $|\psi'\rangle = |\psi\rangle$ in the Mott limit ($S, J = 0$). This yields $E \equiv E[\{f_n\}; J]$ to be

$$\begin{aligned} E = \sum_{\mathbf{r},n}[-\mu n + Un(n-1)/2]|f^{(\mathbf{r})}_n|^2 - J\sum_{\langle \mathbf{r}\mathbf{r}'\rangle}\Big\{&\varphi^*_{\mathbf{r}}\varphi_{\mathbf{r}'} - 2\,\mathrm{Re}\,\varphi^*_{\mathbf{r},\bar{n}-1}\varphi_{\mathbf{r}'\bar{n}} + J\bar{n}(\bar{n}+1)/U \\ &\times\Big[|f^{(\mathbf{r})}_{\bar{n}}|^2|f^{(\mathbf{r}')}_{\bar{n}}|^2 - |f^{(\mathbf{r})}_{\bar{n}+1}|^2|f^{(\mathbf{r}')}_{\bar{n}-1}|^2 - f^{*(\mathbf{r})}_{\bar{n}+1}f^{(\mathbf{r})}_{\bar{n}}f^{*(\mathbf{r}')}_{\bar{n}-1}f^{(\mathbf{r}')}_{\bar{n}+1}\Big] + 2J/U\,\mathrm{Re}\,\Phi^*_{\mathbf{r},\bar{n}-2}\Phi_{\mathbf{r}'\bar{n}}\Big\} \\ - J^2/U\sum_{\langle \mathbf{r}\mathbf{r}'\mathbf{r}''\rangle}\Big\{&2\,\mathrm{Re}\Big[\varphi^*_{\mathbf{r},\bar{n}-1}(\bar{n}+1)|f^{(\mathbf{r}')}_{\bar{n}}|^2 + \varphi_{\mathbf{r}\bar{n}}\Phi^*_{\mathbf{r}',\bar{n}-2} - \varphi^*_{\mathbf{r}\bar{n}}\bar{n}|f^{(\mathbf{r}')}_{\bar{n}-1}|^2 - \varphi_{\mathbf{r},\bar{n}-1}\Phi^*_{\mathbf{r}',\bar{n}-1}\Big]\varphi_{\mathbf{r}''} \\ &+ 2\,\mathrm{Re}\Big[\varphi^*_{\mathbf{r},\bar{n}-1}\Phi_{\mathbf{r}'\bar{n}} + \varphi_{\mathbf{r}\bar{n}}\bar{n}|f^{(\mathbf{r}')}_{\bar{n}}|^2 - \varphi^*_{\mathbf{r}\bar{n}}\Phi_{\mathbf{r}',\bar{n}-1} - \varphi_{\mathbf{r},\bar{n}-1}(\bar{n}+1)|f^{(\mathbf{r}')}_{\bar{n}+1}|^2\Big]\varphi^*_{\mathbf{r}''} \\ &+ \varphi^*_{\mathbf{r}\bar{n}}\bar{n}\Big[|f^{(\mathbf{r}')}_{\bar{n}-1}|^2 - |f^{(\mathbf{r}')}_{\bar{n}}|^2\Big]\varphi_{\mathbf{r}''\bar{n}} + \varphi_{\mathbf{r},\bar{n}-1}(\bar{n}+1)\Big[|f^{(\mathbf{r}')}_{\bar{n}+1}|^2 - |f^{(\mathbf{r}')}_{\bar{n}}|^2\Big]\varphi^*_{\mathbf{r}'',\bar{n}-1} \\ &+ 2\,\mathrm{Re}\,\varphi^*_{\mathbf{r}\bar{n}}\Phi_{\mathbf{r}',\bar{n}-1}\varphi^*_{\mathbf{r}'',\bar{n}-1}\Big\}, \end{aligned} \quad (8)$$

where $\varphi_{\mathbf{r}}[\Phi_{\mathbf{r}}] = \langle\psi'|b_{\mathbf{r}}|\psi'\rangle[\langle\psi'|b^2_{\mathbf{r}}|\psi'\rangle] = \sum_n \varphi_{\mathbf{r}n}[\Phi_{\mathbf{r}n}] = \sum_n \sqrt{n+1}f^{*(\mathbf{r})}_{\mathrm{n}}f^{(\mathbf{r})}_{\mathrm{n}+1}[\sum_n \sqrt{(n+1)(n+2)}f^{*(\mathbf{r})}_{\mathrm{n}}f^{(\mathbf{r})}_{\mathrm{n}+2}]$. Note that the first three terms in the first line of Eq. 8 represent the mean-field energy functional, while the rest are corrections due to quantum fluctuations. The phase diagram obtained by minimizing $E[\{f_n\}; J]$ with respect to $\{f_n\}$ (or by solving $i\hbar\partial_t|\psi'\rangle = H^*[J]|\psi'\rangle$ in imaginary t[25]) for 2D(3D) and $\bar{n} = 1$ is shown in Fig. 1(a) and (b). We note that the match with QMC data[10] is nearly perfect for 3D (Fig. 1(b)) where mean-field theory provides an accurate starting point. While in 3D the accuracy with QMC at the tip of the Mott lobe is $\sim 0.05\%$, in 2D we find $J_c/U = 0.055$ compared to the QMC value 0.061 (red line in Fig. 1(a)). Here the match with QMC is not as accurate as in

3D; however it compares favorably to other analytical methods.[‡] For the rest of this work, we shall restrict ourselves to $d = 3$ and $\bar{n} = 1$ for brevity.

We now apply this method to address the dynamics of the model after a sudden quench from J_i (Mott phase) to J_f (superfluid phase) through the tip of the Mott lobe where the dynamical critical exponent $z = 1$. To solve the Schrödinger equation $i\hbar\partial_t|\psi\rangle = H|\psi\rangle$, we make the transformation $|\psi'\rangle = \exp(iS[J_f])|\psi\rangle$ leading to $i\hbar\partial_t|\psi'\rangle = H^*[J_f]|\psi'\rangle$. Here $|\psi'(t = 0)\rangle$ is the ground state of $H^*[J_i]$ as determined by minimization of $E[\{f_n\}; J_i]$. From this, we obtain the set of coupled equations for $f_n^{(\mathbf{r})}$: $i\hbar\partial_t f_n^{(\mathbf{r})}(t) = \delta E[\{f_n(t)\}; J_f]/\delta f_n^{*(\mathbf{r})}$. The time evolution of the order parameter $\Delta_{\mathbf{r}}(t) = \langle\psi(t)|b_{\mathbf{r}}|\psi(t)\rangle = \langle\psi'(t)|b'_{\mathbf{r}}|\psi'(t)\rangle$, where $b'_{\mathbf{r}} = \exp(iS[J_f])b_{\mathbf{r}}\exp(-iS[J_f])|\psi'(t)\rangle$ can then be expressed in terms of $f_n^{(\mathbf{r})}$ as

$$\begin{aligned}\Delta_{\mathbf{r}}(t) = \varphi_{\mathbf{r}}(t) + J/U\sum_{\langle\mathbf{r}'\rangle_{\mathbf{r}}}\bar{n}\left[|f_{\bar{n}}^{(\mathbf{r})}|^2 - f_{\bar{n}-1}^{(\mathbf{r})}|^2\right]\varphi_{\mathbf{r}'\bar{n}} \\ + (\bar{n}+1)\left[|f_{\bar{n}}^{(\mathbf{r})}|^2 - f_{\bar{n}+1}^{(\mathbf{r})}|^2\right]\varphi_{\mathbf{r}',\bar{n}-1} \\ + \left[\Phi_{\mathbf{r},\bar{n}-2} - \Phi_{\mathbf{r},\bar{n}-1}\right]\varphi^*_{\mathbf{r}'\bar{n}} \\ + \left[\Phi_{\mathbf{r}\bar{n}} - \Phi_{\mathbf{r},\bar{n}-1}\right]\varphi^*_{\mathbf{r}',\bar{n}-1}. \qquad (9)\end{aligned}$$

Note that the first term in Eq. 9 represents the mean-field result. The role of quantum fluctuations in the evolution of $\Delta_{\mathbf{r}}(t)$ becomes evident in computing the equal-time order parameter correlation function $C_{\mathbf{r}}(t) = \langle\psi'(t)|b'_{\mathbf{r}}b'_{\mathbf{r}}|\psi'(t)\rangle - \Delta^2_{\mathbf{r}}(t)$. To compute $\Delta_{\mathbf{r}}$ and $C_{\mathbf{r}}$, we consider a spatially homogeneous system and solve the Schrödinger equation for $f_n^{(\mathbf{r})} \equiv f_n$ (as guaranteed by translational invariance) keeping all states for $0 \le n \le 5$ with $\bar{n} = 1$. The resultant plot of $\Delta_{\mathbf{r}}(t) \equiv \Delta(t)$ is shown in Fig. 2(a)[(d)] for $J_i = 0$ and $J_f/J_c = 1.02(J_f/J_c = 3.51)$. We find that near the critical point, $\Delta(t)$ displays oscillations with a single characteristic frequency[20] while away from the critical point ($J_f/J_c = 3.51$), multiple frequencies are involved in its dynamics. The time period T (Fig. 2(c)) of these oscillations near J_c is found, as a consequence of critical slowing down, to have a divergence $T \sim (\delta J)^{-0.35\pm0.05}$ leading to $z\nu = 0.35 \pm 0.05$ for $d = 3$.[12] Finally, we plot $C_{\mathbf{r}}(t) \equiv C(t)$ as a function of t for $J_f = 1.02J_c$ in Fig. 2(b). We find that $|C(t)/\Delta^2(t)|$ may be as large as 0.5 at the tip of the peaks of $\Delta(t)$, which shows strong quantum fluctuations near the QCP.

Next, we compute the wavefunction overlap $F = |\langle\psi_f|\psi_c\rangle|^2 = |\langle\psi'_f|e^{iS[J_f]}e^{-iS[J_c]}|\psi'_c\rangle|^2$ for sudden quench starting at the QCP. Here $\psi_f(\psi_c)$ denotes the ground state wavefunction for $J = J_f(J_c)$. The residual energy $Q = \langle\psi_c|\mathcal{H}[J_f]|\psi_c\rangle - E_G[J_f]$, where $E_G[J_f]$ denotes the ground state energy at $J = J_f$ as obtained by minimizing E in Eq. 8, can also be computed in a similar manner. Using the fact that for $|\psi'_c\rangle = e^{iS[J_c]}|\psi_c\rangle$, $\varphi_{\mathbf{r}} = \Phi_{\mathbf{r}} = 0$, we find, in terms of the coefficients $f_n^{(\mathbf{r})}$,

$$\begin{aligned}Q = E_G[J_c] - E_G[J_f] - 2J\delta J\bar{n}(\bar{n}+1) \\ \times\sum_{\langle\mathbf{r}\mathbf{r}'\rangle}\left[|f_{\bar{n}}^{(\mathbf{r})}|^2|f_{\bar{n}}^{(\mathbf{r}')}|^2 - |f_{\bar{n}+1}^{(\mathbf{r})}|^2|f_{\bar{n}-1}^{(\mathbf{r}')}|^2\right. \\ \left. - f_{\bar{n}+1}^{*(\mathbf{r})}f_{\bar{n}-1}^{(\mathbf{r})}f_{\bar{n}-1}^{*(\mathbf{r}')}f_{\bar{n}+1}^{(\mathbf{r}')}\right]/U.\end{aligned}$$

A plot of $1 - F$ and Q for the homogeneous case, as a function of δJ for $\delta J/J_c \lesssim 0.2$ is shown in Fig. 3. A numerical fit of these curves yields $1 - F \sim \delta J^{0.89}$ and $Q \sim \delta J^{1.90}$ which disagrees with the universal scaling exponents ($1 - F \sim \delta J^{d\nu}$ and $Q \sim \delta J^{(d+z)\nu}$) expected from sudden dynamics across a QCP with $z = 1$.[28]

To understand the reason for this non-universality, and to address the dynamics of the system during a ramp with finite rate τ^{-1}, we consider ramp process under which J evolves from J_i at $t_i = 0$ to J_f at $t_f = \tau$:$J(t) = J_i + (J_f - J_i)t/\tau$. To solve the Schrödinger equation $i\hbar\partial_t|\psi\rangle = \mathcal{H}[J(t)]|\psi\rangle$, we make a time-dependent transformation $|\psi'\rangle = \exp(iS[J(t)])|\psi\rangle$, which eliminates $T^0_\ell[J(t)]$ up to first order from $\mathcal{H}[J(t)]$ at each instant, and leads to the effective Hamiltonian $H^*[J(t)] = \exp(iS[J(t)])\mathcal{H}[J(t)]\exp(-iS[J(t)])$. This yields the equation $(i\hbar\partial_t + \partial S/\partial t)|\psi'\rangle = H^*[J(t)]|\psi'\rangle$. The additional term $\partial S/\partial t$ takes into account the possibility of creation of excitations during the time evolution with a finite ramp rate τ^{-1}. The above equation yields an accurate description of the ramp with $H^*[J(t)]$ given by Eq. 7 for $J(t)/U \ll 1$. Note that this does not impose a constraint on magnitude of τ; it only restricts J_f/U and J_i/U to be small. Thus the method can treat both "slow" and "fast" ramps at equal footing. Substituting $|\psi'\rangle = \prod_{\mathbf{r}}\sum f_n^{(\mathbf{r})}|n\rangle$, we obtain a set of coupled equations for the coefficients $\{f_n\}$

$$\begin{aligned}i\hbar\partial_t f_n^{(\mathbf{r})} = \delta E[\{f_n(t)\}; J(t)]/\delta f_n^{*(\mathbf{r})} + i\hbar\frac{(J_f - J_i)}{U\tau} \\ \times\sum_{\langle\mathbf{r}'\rangle_{\mathbf{r}}}\sqrt{n}f_{n-1}^{(\mathbf{r})}\left[\delta_{n\bar{n}}\varphi_{\mathbf{r}'\bar{n}} - \delta_{n,\bar{n}+1}\varphi_{\mathbf{r}',\bar{n}-1}\right] \\ + \sqrt{n+1}\,f_{n+1}^{(\mathbf{r})}\left[\delta_{n\bar{n}}\varphi^*_{\mathbf{r}',\bar{n}-1} - \delta_{n,\bar{n}-1}\varphi^*_{\mathbf{r}'\bar{n}}\right]. \qquad (10)\end{aligned}$$

[‡]See for example, M. Lewenstein, A. Sanpera, V. Ahufinger, B. Damskic, A. Sen(De) and U. Sen Adv. Phys. **56**,243 (2007).

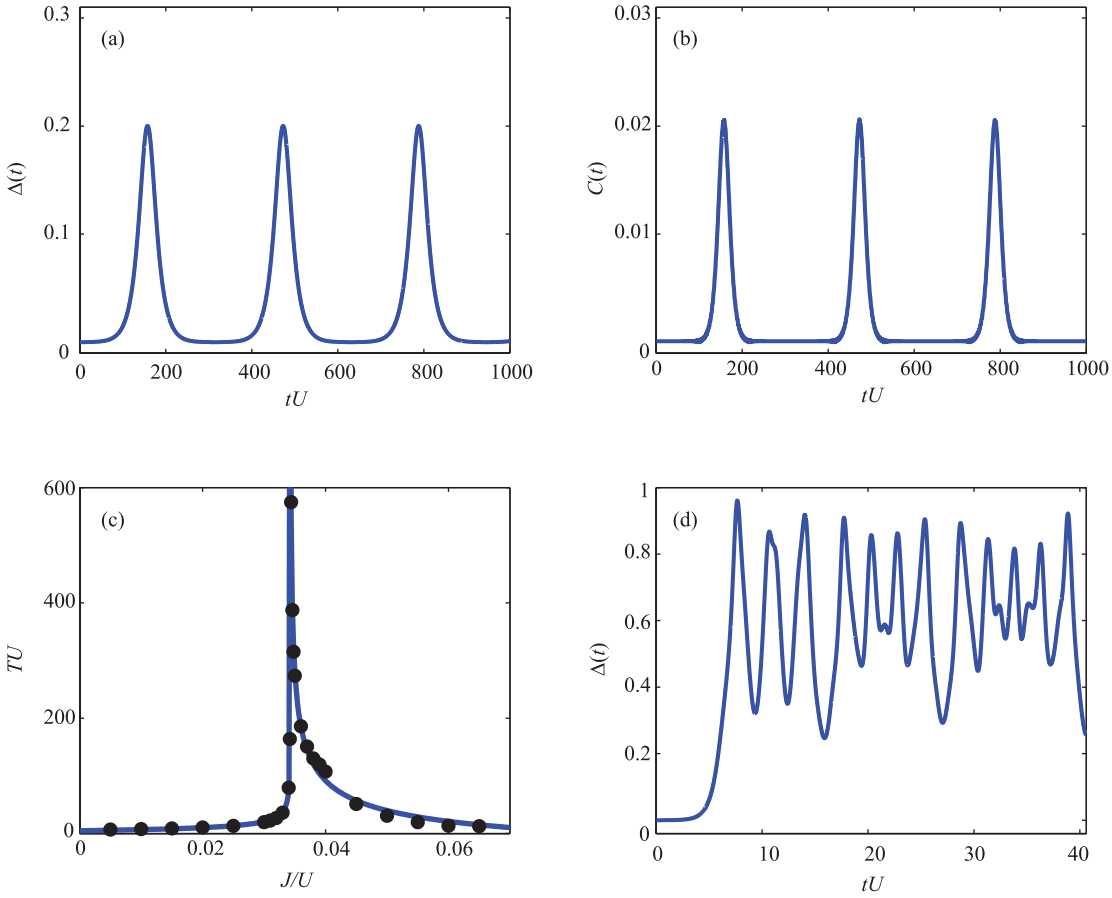

Figure 2: (Color online) Plot of $\Delta(t)$ (a), and $C(t)$ (b) as a function of tU, for $J_f = 1.02J_c$. (c) The time period T of the oscillations of $\Delta(t)$. (d) Same as in (a) for $J_f = 3.51J_c$. We have set $\hbar = 1$ for all plots.

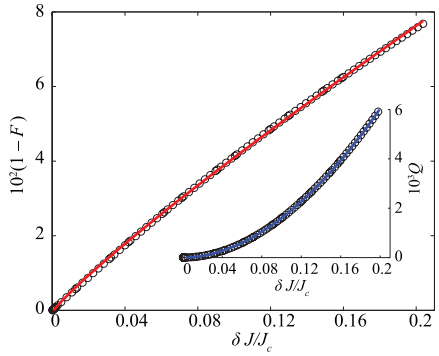

Figure 3: (Color online) Plot of F and Q as a function of the δJ for $\delta J/J_c \ll 1$. The lines correspond to fits yielding a power $1 - F(Q) \sim (\delta J)^{r_1(r_2)}$ with $r_1 \simeq 0.89$ and $r_2 \simeq 1.9$.

Using Eq. 10, we solve for $f_n^{(\mathbf{r})} \equiv f_n$ for translationally invariant systems and compute the defect density $P = 1 - |\langle\psi_G|\psi(t_f)|^2$, where $|\psi_G\rangle$ ($|\psi(t_f)\rangle$) denotes the final ground state (state after the ramp), for a ramp from $J_i/U = 0.05$ (superfluid phase) to $J_f/U = 0.005$ (Mott phase) as a function of τ. We find that P exhibits a plateau like behavior at large τ, and do not display universal scaling as expected from generic theories of slow dynamics of quantum systems near critical point.[12] This seems to be in qualitative agreement with the recent experiments presented in Ref.[2], where ramp dynamics of ultracold bosons from superfluid to the Mott region has been experimentally studied. Indeed, it was found, via direct measurement of $\bar{n}$ per site, that P displays a plateau like behavior similar to Fig. 4(a) [the inset displays the saturation for longer τ]. In Fig. 4(b), we show the analogous saturation of Q as a function of τ. The inset of Fig. 4(b) shows Q and $1 - F$ as a function of δJ for $\tau = \hbar/U$ with $J_i = J_c$. These plots yields exponents nearly identical to those obtained from Fig. 3 reflecting reproduction of the sudden quench limit.

Such a lack of universality in the dynamics can be qualitatively understood from absence of contribution of the critical ($\mathbf{k} = 0$) modes. In the strong-coupling regime ($zJ/U \ll 1$), the system can access the $\mathbf{k} = 0$ modes after time $\mathcal{T}$ which can

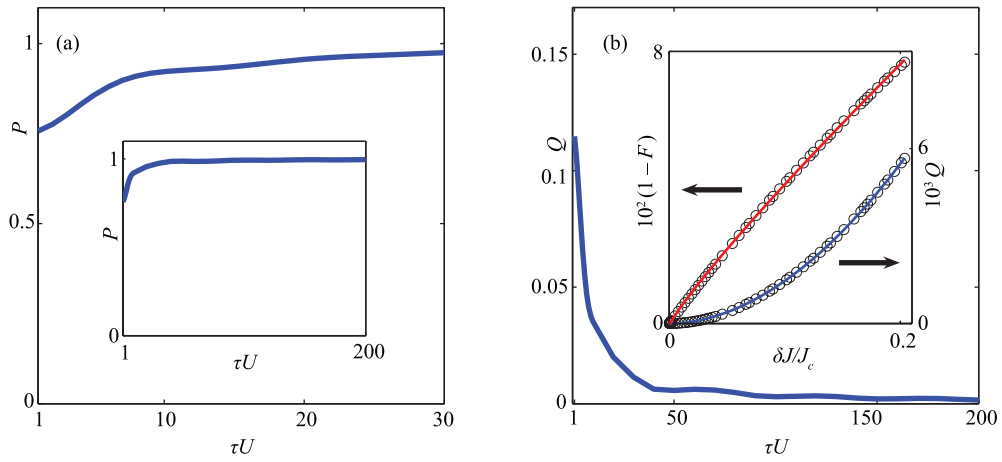

Figure 4: (Color online) (a) Plot of P as a function τU (in units of $\hbar = 1$) for $J_i/U = 0.05$ (SF phase) and $J_f/U = 0.005$ (Mott phase) showing the plateau-like behavior at large τ, and the corresponding saturation of Q (b). The inset in (b) shows Q and $1 - F$ as a function of $\delta J/J_c$ for $\tau U = 1$.

be roughly estimated as the time taken by a boson to cover the linear system dimension L. For typical small J ($U = 1$) in the Mott phase and near the QCP, $\mathcal{T} \sim \mathrm{O}(L\hbar/J)$ can be very large. Thus for $t \leq \mathcal{T}$, the dynamics, governed by local physics which is well captured by our method, do not display critical scaling behavior. We note that in realistic experimental setups in the deep Mott limit,[2] $\mathcal{T}$ may easily exceed the system lifetime making observation of universal scaling behavior impossible in such setups.

In conclusion, we have provided a brief introduction to the dynamics of ultracold bosons near the superfluid-insulator quantum critical point using a semi-analytical projection operator method which is the only available method for studying such dynamics beyond mean-field theory for $d > 1$. The qualitative predictions of this method matches with what is seen in recent experiments.[2] A possible extension of these studies would be to use this method for studying dynamics multi-species bosons, and for bosons in a trap or in the presence of disorder.

Received 8 May 2014.

References

1. M. Greiner, O. Mandel, T. Esslinger, T. W. Hänsch1 and I. Bloch Nature **415**, 39 (2002); C. Orzel, A. K. Tuchman, M. L. Fenselau, M. Yasuda and M. A. Kasevich, Science **291**, 2386 (2001); T. Kinoshita, T. Wenger, and D. S. Weiss, Nature **440**, 900 (2006); L. E. Sadler, J. M. Higbie, S. R. Leslie, M. Vengalattore and D. M. Stamper-Kurn, Nature **443**, 312 (2006).
2. W. S. Bakr, A. Peng, M. E. Tai, R. Ma, J. Simon, J. I. Gillen, S. Folling, L. Pollet, and M. Greiner, Science **329**, 547 (2010).
3. D. Jaksch, C. Bruder, J. I. Cirac, C. W. Gardiner, and P. Zoller, Phys. Rev. Lett. **81**, 3108 (1998).
4. M. P. A. Fisher, P. B. Weichman, G. Grinstein, and D. S. Fisher, Phys. Rev. B **40**, 546 (1989).
5. K. Sheshadri, H. R. Krishnamurthy, R. Pandit, and T. V. Ramakrishnan, Europhys. Lett. **22**, 257 (1993).
6. J. K. Freericks and H. Monien, Europhys. Lett. **26**, 545 (1994); *ibid*, Phys. Rev. B **53**, 2691 (1996).
7. W. Krauth and N. Trivedi, Europhys. Lett. **14**, 627 (1991).
8. K. Sengupta and N. Dupuis, Phys. Rev. **71**, 033629 (2005).
9. A. Rancon and N. Dupuis, Phys. Rev. B **83**, 172501 (2011); *ibid.*, Phys. Rev. B **84**, 174513 (2011).
10. B. Caprogrosso-Sansone, N. Prokofev, and B. V. Svistunov, Phys. Rev. B **75**, 134302 (2007).
11. J. K. Freericks, H. R. Krishnamurthy, Y. Kato, N. Kawashima, and N. Trivedi, Phys. Rev. A **79**, 053631 (2009).
12. A. Polkovnikov, K. Sengupta, A. Silva, and M. Vengalattore, Rev. Mod. Phys. **83**, 863 (2011); J. Dziarmaga, Adv. Phys. **59**, 1063 (2010).
13. A. Polkovnikov, Phys. Rev. B **72**, 161201(R) (2005).
14. K. Sengupta, D. Sen, and S. Mondal, Phys. Rev. Lett. **100**, 077204 (2008); S. Mondal, D. Sen, and K. Sengupta, Phys. Rev. B **78**, 045101 (2008).
15. D. Sen, K. Sengupta, and S. Mondal, Phys. Rev. Lett. **101**, 016806 (2008); S. Mondal, K. Sengupta, and D. Sen, Phys. Rev. B **79**, 045128 (2009).
16. F. Pellegrini, S. Montangero, G. E. Santoro, and R. Fazio, Phys. Rev. B **77**, 140404(R) (2008); U. Divakaran, A. Dutta, and D. Sen, *ibid.* **78**, 144301 (2008); U. Divakaran, V. Mukherjee, A. Dutta, and D. Sen, J. Stat. Mech. (2009) P02007.
17. C. Kollath, A. Lauchli, and E. Altman, Phys. Rev. Lett. **98**, 180601 (2007).
18. C. De Grandi, V. Gritsev, A. Polkovnikov, Phys. Rev. B **81**, 224301 (2010); C. De Grandi, R. A. Barankov, and A. Polkovnikov, Phys. Rev. Lett. **101**, 230402 (2008).

19. A. Polkovnikov, Phys. Rev. **66**, 053607 (2002); A. Polkovnikov and V. Gritsev, Nat. Phys. **4**, 477 (2006).
20. E. Altman and A. Auerbach, Phys. Rev. Lett. **89**, 250404 (2002).
21. M. P. Kennett and D. Dalidovich, Phys. Rev. A **84**, 033620 (2011).
22. R. Schützhold, M. Uhlmann, Y. Xu, and U. R. Fischer, Phys. Rev. Lett. **97**, 200601 (2006); J. Wernsdorfer, M. Snoek, and W. Hofstetter Phys. Rev. **81**, 043620 (2010).
23. C. Trefzger and K. Sengupta, Phys. Rev. Lett. **106**, 095702 (2011).
24. A. Isacsson, Min-Chul Cha, K. Sengupta, and S. M. Girvin, Phys. Rev. B **72**, 184507 (2005).
25. C. Trefzger, C. Menotti, and M. Lewenstein, Phys. Rev. **78**, 043604 (2008).
26. R.V. Pai, R. Pandit, H.R. Krishnamurthy, and S. Ramasesha, Phys. Rev. Lett. **76**, 2937 (1996); T. D. Kuhner and H. Monien, Phys. Rev. B **58**, 14741 (1998); T. D. Kuhner, S.R. White, and H. Monien, Phys. Rev. B **61**, 12474 (2000).
27. K. V. Kruititsky and P. K. Navez, Phys. Rev. **84**, 033602 (2011).
28. C. De Grandi, V. Gritsev, and A. Polkovnikov, Phys. Rev. B **81**, 012303 (2010); C. de Grandi and A. Polkovnikov, *Quantum Quenching, Annealing and Computation*, Eds. A. Das, A. Chandra and B. K. Chakrabarti, Lect. Notes in Phys., **802** (Springer, Heidelberg 2010).
29. F. Gerbier, Phys. Rev. Lett. **99**, 120405 (2007); D. M. Weld, P. Medley, H. Miyake, D. Hucul, D. E. Pritchard, and W. Ketterle, Phys. Rev. Lett. **103**, 245301 (2009).

Krishnendu Sengupta is a theoretical condensed matter physicist whose research focuses on quantum phase transition, non-equilibrium dynamics, properties of ultracold atoms, and topological materials such as graphene and topological insulators. He has a Ph.D. from University of Maryland (2001), did his postdoctoral works at Yale (2001–2004) and Toronto (2004–2005), and is currently a professor in the theoretical physics department at the Indian Institute of Science in Kolkata.